frontiers | Frontiers in Acoustics

TYPE Original Research
PUBLISHED 08 November 2024
DOI 10.3389/facou.2024.1478414

OPEN ACCESS

EDITED BY
Andrea Santoni,
University of Ferrara, Italy

REVIEWED BY
Antonio Petošić,
University of Zagreb, Croatia
Arnaud Duval,
Treves Product Services & Innovation, France
Walid Larbi,
Conservatoire National des Arts et Métiers (CNAM), France

*CORRESPONDENCE
Julien Biboud,
julien.biboud@mecanum.com

RECEIVED 09 August 2024
ACCEPTED 23 October 2024
PUBLISHED 08 November 2024

CITATION
Biboud J, Elkoun S and Panneton R (2024) Optimization of sound absorption of recycled Nylon fibrous materials.
Front. Acoust. 2:1478414.
doi: 10.3389/facou.2024.1478414

Optimization of sound absorption of recycled Nylon fibrous materials

Julien Biboud[1,2]*, Saïd Elkoun[1] and Raymond Panneton[1]

[1]CRASH, Centre de Recherche Acoustique-Signal-Humain, Université de Sherbrooke, Sherbrooke, QC, Canada, [2]Mecanum Inc., Sherbrooke, QC, Canada

A semi-empirical model for the assessment and an optimization procedure of the sound absorption coefficient of compressed nonwoven fibrous materials made from recycled Nylon fibers (RNF) is developed. In general, the prediction of the sound absorption properties of materials requires the measurement of non-acoustic parameters by specialized characterization tools that are not always within reach of most laboratories. The objective of the proposed model is to establish empirical relationships between these non-acoustic parameters and the bulk density of RNF materials. These empirical relationships are then substituted into a conventional acoustic model for porous materials, namely, the model of Johnson-Champoux-Allard. The proposed model accurately predicts the sound absorption coefficients of compressed RNF materials based solely on bulk density, thickness, and frequency. This prediction is validated through impedance tube measurements. Moreover, the model is used with a proposed optimization producedure to identify the ideal density and thickness for maximum sound absorption at a specific frequency. Impedance tube measurements on optimized configurations confirm the effectiveness of this optimization process.

KEYWORDS

sound absorption, optimization, recycled fibers, nonwoven, fibrous, bulk density

1 Introduction

In the current context of sustainable development, engineers and scientists are developing materials having a minimum impact on the environment; they are called green or eco-friendly materials. Some of these materials have shown excellent sound absorption properties compared to conventional materials such as glass and rock wools, with a minimum impact on the environment. In fact, while glass and rock wools are excellent sound absorbers, their recycling is still difficult and their processing is highly energy-consuming (Desarnaulds et al., 2005). An alternative to these wools are fibrous materials made from recycled fibers–this paper focuses on this type of materials. Such materials already replaced successfully glass and rock wools: cotton absorbers made from recycled clothing (shoddies) (Langley et al., 2000) and cellulose insulation made from recycled newspapers and even vegetal wools (Piégay et al., 2021) are a few examples. Reviews of sustainable materials and their applications to noise control can be found elsewhere (Desarnaulds et al., 2005; Langley et al., 2000; Asdrubali, 2006).

The modeling of sound propagation and sound dissipation in traditional porous materials is well known. Reviews can be found elsewhere for fibrous materials (Manning and Panneton, 2013; Lei et al., 2018; Tran et al., 2024a) and general porous media (Allard and Atalla, 2009). For eco-friendly acoustic fibrous materials made from

recycled materials, many research works have been published in the past 10 years. Most of these works focus on the characterization of their acoustic properties (ex.: sound absorption coefficient) and on the comparison with traditional glass or mineral wools (Manning and Panneton, 2013; Lorenzana et al., 2002; Lee and Joo, 2003; Kosuge et al., 2005; D'Alessandro and Pispola, 2005; Del Rey et al., 2011; Maderuelo-Sanz et al., 2012). These works show the potential of using fibers from different post-consumer or post-industrial wastes (end-of-life tires, plastic bottles, used carpets, metal shavings, fabrics ...) to fabricate good fibrous sound absorbers. In these works, most of the recycled fibrous materials are nonwoven assemblies, where the fibers are blended and mechanically bonded (ex.: needle punched), thermally bonded or resin bonded. In general, few details are given to link their acoustic performance to their fabrication process, their microstructure or intrinsic parameters with a view to optimizing their sound absorption properties.

Porous materials are frequently acoustically modeled using an equivalent fluid method, assuming the frame is acoustically rigid. Common models for this approach include the 6-parameter Johnson-Lafarge (JL) model and the 5-parameter Johnson-Champoux-Allard (JCA) model. The parameters for these models are static airflow resistivity, open porosity, tortuosity, viscous and thermal characteristic lengths, and static thermal permeability. In the past, numerous theoretical and numerical studies have been conducted to connect these parameters for fiber bundles to their microstructure and acoustic properties, with reviews available elsewhere. (Luu et al., 2017; Pompoli and Bonfiglio, 2020; Tran et al., 2024a) However, such research on acoustic materials made from waste textiles or natural fibers remains limited.

Manning and Panneton (2013) measured the JL parameters in various manufactured samples of shoddies made from waste textiles. They developed empirical formulas that relate the JL parameters to the bulk densities of shoddies, which range from 30 to 180 kg/m^3 (or porosity from 86% to 98%), with an average fiber diameter of about 22 μ m. (Manning and Panneton, 2013) Santoni et al. introduced an effective fluid dynamic fiber radius for sound insulation materials made from natural hemp fibers. This diameter, derived from an analytical expression of airflow resistivity and its measurement, ranges between 18 and 27 μ m for the manufactured samples. Except for the viscous characteristic length, which is determined by inversion on an acoustic measurement, existing expressions were used to link the other JCA parameters to this effective fiber radius and bulk density. They applied a homothety law to recalculate all JCA parameters across different compression ranges, covering bulk densities from 50 to 150 kg/m^3 (or porosity from 88% to 96%). (Santoni et al., 2019).

For felts made from recycled fibers, Tran et al. used a multiscale numerical approach to link the microstructural features (fiber radius distributions and orientation) to the JL parameters. From their results, they updated the semi-analytical relations of Luu et al. (valid for a single fiber diameter) by including the fiber diameter distribution. Contrary to the latter two studies, this time the relations are based only on microstructural features and not on the bulk density. Also, their relations are validated for fiber diameters varying between 0 and 60 μ m following a Gamma function distribution, and porosity from 65% to 99%. (Tran et al., 2024b). In a subsequent paper, Tran et al. utilized these relations as a basis for optimization, employing an iterative differential evolution algorithm to enhance sound absorption. (Tran et al., 2024a).

All the previous relations on sustainable materials were experimentally validated against measured JL or JCA parameters and their ability to predict the normal incidence sound absorption coefficient obtained using an impedance tube. A common aspect of these studies is that the average diameter of the fibers is less than 30 μ m. Moreover, these studies did not address the optimization of the material for sound absorption by a direct method (i.e., not iterative). In this study, the sound absorption coefficient of nonwoven blends made from a Recycled Nylon Fibers (RNF) derived from carpet waste is investigated. Contrary to the previous studies, the diameter of the fibers is much lager and range between 50 and 90 μ m. Consequently, the main purpose of this work is to propose a robust semi-empirical model to predict and optimize the sound absorption of a RNF blend with only one physical parameter, the bulk density. A general direct optimization approach inspired by the non-dimensional design charts for fibrous sound absorbers by Mechel (Mechel, 1988) is proposed. While this direct optimization approach is developed for the studied RNF nonwoven, it could be extended to any other types of porous materials.

In the following, the acoustic model used to describe the porous materials is first presented. Second, experimental characterizations of several RNF assemblies of different densities, ranging from 30 to 180 kg/m^3;, are performed. Empirical relationships between each material property (airflow resistivity, open porosity, tortuosity, viscous and thermal characteristic lengths) and the bulk density are developed. Third, the empirical relationships are used in the acoustic model to derive the semi-empirical model for the RNF blend. This semi-empirical model depends only on the bulk density and thickness of the blend, and the frequency. Fourth, design charts for the RNF sound absorbers are obtained from the semi-empirical model to define optimal sound absorption configurations. To facilitate optimization, a straightforward theoretical procedure is finally developed and validated.

2 Theory

The RNF blend is seen as a porous medium made of a solid phase (the fibers) and a fluid phase (here air), see Figure 1. The fluid phase forms a complex network of interconnected pores in which an acoustic wave can propagate and dissipate by thermal and viscous losses. Typically, the fluid phase network is characterized by five macroscopic parameters. Besides the bulk density (ρ_B), these parameters are the open porosity (ϕ), the static airflow resistivity (σ), the tortuosity (α_∞), the viscous characteristic length (Λ), and the thermal characteristic length (Λ'). These parameters are homogeneous at the macroscopic scale H defined in Figure 1. This scale is much larger than the diameter of the fibers, and much smaller than the wavelength λ of the acoustical wave. The macroscopic parameters are used to populate an acoustical propagation model based on an equivalent fluid approach (Panneton, 2007). Following this approach, the elastic deformation of the solid phase is neglected and only sound pressure waves propagate in the fluid network. The sound pressure p in this equivalent fluid is governed by the homogeneous Helmholtz equation

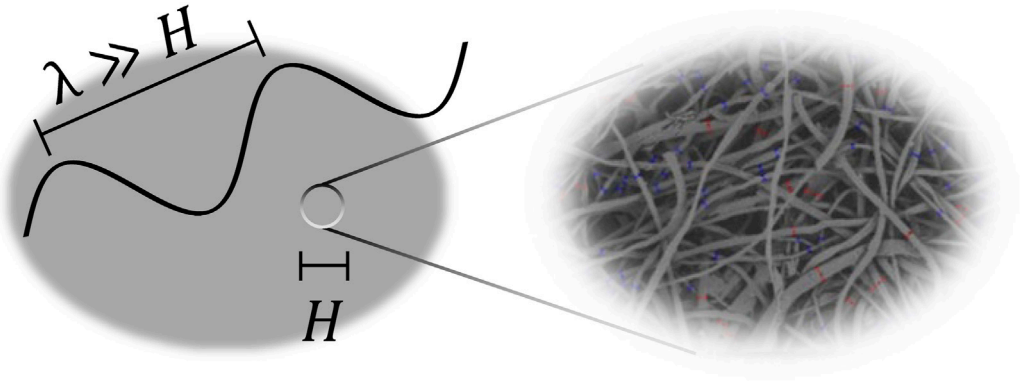

FIGURE 1
Representation of the acoustic macroscopic scale H on a material sample (large gray disk), where λ is the wavelength of the acoustic phenomenon. The dashed circle represents the smallest area on which an acoustic property (porosity, resistivity, etc.) is homogeneous over the surface.

$$\Delta p + (2\pi f)^2 \frac{\rho_{eq}}{K_{eq}} p = 0 \tag{1}$$

where f is the frequency in Hertz, Δ is the Laplacian operator, and ρ_{eq} and K_{eq} are the equivalent dynamic density and the equivalent dynamic bulk modulus of the equivalent fluid. In Equation 1, both equivalent properties are frequency-dependent and complex-valued to account for the viscous and thermal losses, respectively. Many models exist to predict these two equivalent properties. A review is given elsewhere. (Allard and Atalla, 2009) In engineering applications dealing with sound-absorbing porous materials, the Johnson-Champoux-Allard (JCA) model is largely used. This model is well adapted to most open-cell porous materials, without being limited to specific high porosity fibrous materials with a given fiber size distribution (ex.: mineral wool based model by Delany and Bazley (1970)). Moreover, it depends on measurable parameters only.

In the present work, the acoustic response of the RNF blend may differ from the classical behavior of simple fiber assemblies, more particularly at higher compaction levels (i.e., higher densities, lower porosities, and higher tortuosities). Consequently, it is preferred to use the general 5-parameter JCA model instead of a specific model. In this model, the equivalent dynamic density and bulk modulus are given by (Equations 5 of Allard and Atalla (2009))

$$\rho_{eq}(f) = \frac{\rho_0 \alpha_\infty}{\phi}\left(1 - j\frac{\sigma\phi}{2\pi f \rho_0 \alpha_\infty}\sqrt{1 + j\frac{8\pi f \rho_0 \alpha_\infty^2 \eta}{\sigma^2 \phi^2 \Lambda^2}}\right) \tag{2}$$

and

$$K_{eq}(f) = \frac{\gamma P_0/\phi}{\gamma - (\gamma-1)\left(1 - j\frac{4\eta}{\pi f \rho_0 \mathrm{Pr}\Lambda'^2}\left(1 + j\frac{\pi f \rho_0 \mathrm{Pr}\Lambda'^2}{8\eta}\right)^{1/2}\right)^{-1}} \tag{3}$$

where $j^2 = -1$ and ρ_0, γ, Pr and η are the density, specific heat ratio, Prandtl number, and dynamic viscosity of the saturating fluid, respectively. Note that all the properties defined in this work are in MKS units. For soft fibrous materials (limp materials), it is usually preferred to take into account for the added mass of the fibers by using the corrected dynamic density of the equivalent fluid (Panneton, 2007)

$$\rho'_{eq} = \frac{\rho_{eq}(\rho_B + \phi\rho_0) - \rho_0^2}{\rho_{eq} + \rho_B - \rho_0(2-\phi)}. \tag{4}$$

Once these two dynamic properties are known, the sound absorption coefficient of a layer of thickness L backed by a hard wall is given by

$$\alpha = 1 - \left|\frac{Z_s - \rho_0 c_0}{Z_s + \rho_0 c_0}\right|^2 \tag{5}$$

where c_0 is the speed of sound in the fluid, and Z_s is the acoustic surface impedance

$$Z_s = \sqrt{\rho_{eq} K_{eq}}\,\coth\left(j2\pi f L\sqrt{\frac{\rho_{eq}}{K_{eq}}}\right). \tag{6}$$

2.1 Optimization of sound absorption

The surface impedance in Equation 6 depends on six material parameters (ρ_B, ϕ, σ, α, Λ, Λ'), the thickness and the frequency. If one wants to design a sound absorber with maximum absorption (i.e., α=1) at a given frequency, or for a given thickness, this means that the parameters need to be adjusted (or optimized) so that $Z_s = \rho_0 c_0$. This is possible from a mathematical point of view. However, since the material parameters are all interrelated and related to the structure of the pore network, it may be difficult to find a physical solution. The idea developed in the following is to connect all these material parameters to a single parameter easily identifiable and measurable, namely, the bulk density. This will end in a realistic and pragmatic optimization procedure for maximizing the sound absorption of the blend.

3 Experimental characterization, material and methods

3.1 Description of the materials

The fibers used in this study come primarily from recycled carpets. The carpets are shredded into short fibers which are then

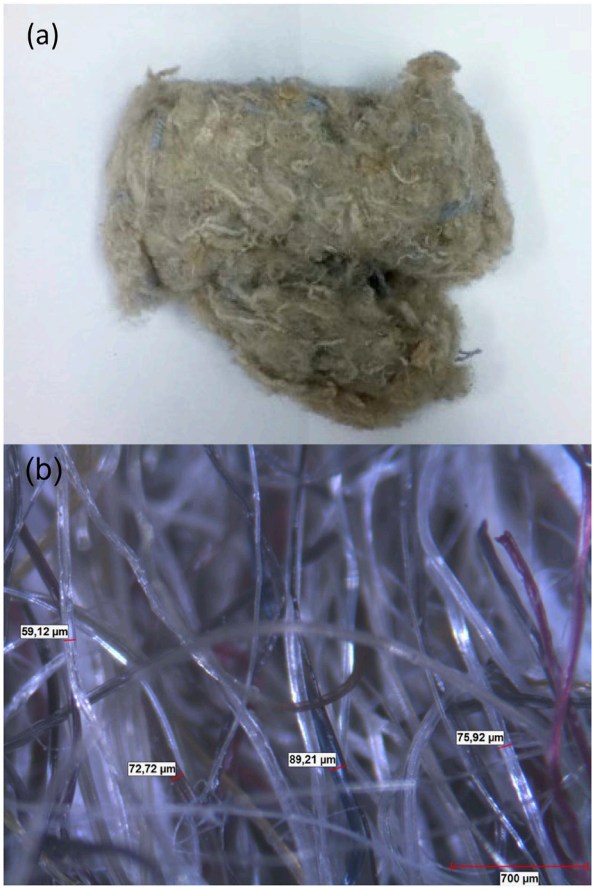

FIGURE 2
(A) Photos of the studied fiber blend made from recycled carpets. **(B)** Optical microscope images. The fiber diameters range generally from 50 to 90 μ m.

cleaned up and mixed into a homogeneous mixture. Finally, the blend is compacted to reach a given bulk density. Figure 2 shows photos of the mixture. An optical analysis indicates that the diameter d of the fibers ranges typically between 50 and 90 μ m. The data provided by the manufacturer indicates that the fiber blend is composed of 80%–85% Nylon, 6%–12% of polypropylene and 6%–8% of residues such as latex and carbonate calcium. It is worth mentioning that no specific bonding method was used. In fact, for the sake of simplicity, the blend was only compacted between a grid and the hard termination of an impedance tube, see Figure 3. As noted by Lee and Joo (2003), they observed that the web properties after needling were insignificant on the sound absorption of the fiber agglomerates. Also, results obtained from Maderuelo-Sanz et al. (2012) (see their results for samples M-B and M-C, Figure 4 showed that resin impregnation had little effect on the sound absorption of their recycled fiber assemblies. While in some cases the bonding method may influence sound absorption (Manning and Panneton, 2013), it can be assumed that its impact can be indirectly addressed by the bulk density of the agglomerate, provided that the agglomerate remains flexible or soft. Therefore, in this work, no special attention is paid to the bonding method.

3.2 Sound absorption coefficient (α)

The normal incidence sound absorption coefficient of a test specimen is measured following the standard test method ISO 10534-2 using a Mecanum's impedance tube with the transfer-function method. (ISO 10534–2:2023, 2023) A tube of D = 44.44 mm in diameter is used. The valid frequency range of the tube spans from 100 Hz to 4,100 Hz. To test RNF blends at different bulk densities, a given mass M of RNF is compacted in the tube between a fixed grid and the hard termination of the tube, see Figure 3. The grid is acoustically transparent and the thickness of the blends is fixed to L = 50 mm. The bulk density of a compacted RNF blend is then given by $\rho_B = 4M/\pi D^2 L$.

3.3 Bulk density (ρ_B) and fiber density (ρ_f)

From the fiber composition detailed above, one can estimate the density of a representative fiber of the blend by $\hat{\rho}_f = \sum w_i \rho_{fi}$, where ρ_{fi} is the density of constituent i (i = nylon, polypropylene, residues) and w_i its proportion in the blend. Applying this formula, one finds $\hat{\rho}_f$ = 1,114.8 12.5 kg/m^3;. To check this value, an open porosity test, with a Mecanum's porosity and density meter, was performed on 8 samples following a pressure/mass method (Salissou and

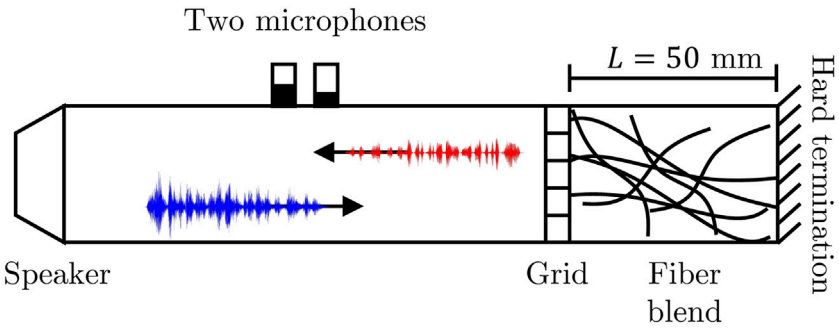

FIGURE 3
Sketch of the impedance tube with the fiber blend compacted between the grid and the hard wall termination.

FIGURE 4
Specimen holder placed in the support of the airflow resistivity meter [Model Sigma-X 2010, Mecanum, inc.].

Panneton, 2007). In this method, using a 10-mg readability balance, the mass of an empty test chamber of 1,161 cm^3; is measured at low absolute pressure (0.1 psi) and at high absolute pressure (approximately 91.5 psi) when pressurized with argon. The same measurements are repeated when the test chamber is filled with approximately 93.5 g of compacted fiber blend. With the four measured masses, and using the perfect gas law, the method yields an open porosity of ϕ = 0.926 ± 0.001 and a bulk density of ρ_B= 80.53 ± 0.01 kg/m^3;. The measured open porosity represents the interconnected air volume in the tested compacted blend (i.e., the air phase) seen by an acoustical wave propagating in the porous medium. The measured bulk density of the compacted blend is given by the in-vacuum mass of the blend divided by its bulk volume (here the test chamber volume). From the measured open porosity and bulk density, one can determine the representative fiber density from the following relation

$$\rho_f = \frac{\rho_B}{1-\phi} \tag{7}$$

With the measured values on 8 samples, this yields ρ_f =1,094.13 19.38 kg/m^3;. This result is in accordance with the one estimated above from the composition of the blend. This value will be used in this work. Results of individual measurements are summarized in Table 1. Note that in this study, all parameter variations are expressed as standard deviations.

3.4 Open porosity (ϕ)

Since the measurement of the open porosity is lengthy, one prefers to use Equation 7 to deduce the porosity of a given compaction of fibers. For the sake of clarity, Equation 7 is rewritten in terms of open porosity in function of bulk density

TABLE 1 Results of the porosity and bulk density tests using the pressure/mass method. The fiber density (last column) is deduced from Equation 7.

Samples	ϕ	ρ_B, kg/m^3	ρ_f,kg/m^3
# 1	0.926	80.5	1,088.2
# 2	0.927	80.5	1,103.0
# 3	0.928	80.5	1,118.3
# 4	0.928	80.5	1,118.5
# 5	0.924	80.5	1,059.7
# 6	0.926	80.5	1,088.4
# 7	0.927	80.5	1,103.2
# 8	0.925	80.5	1,073.7

$$\phi(\rho_B) = 1 - \frac{\rho_B}{\rho_f}. \tag{8}$$

This equation assumes knowledge of the representative density of the fibers.

3.5 Static airflow resistivity (σ)

The static airflow resistivity σ of a material is defined as its ability to hinder or block airflow. Its measurement is carried out using a Mecanum's Airflow resistance meter which follows the direct airflow method of ISO 9053-2 standard test method for airflow resistance of acoustical materials. (ISO 9053–2:2020, 2020) It is given by

$$\sigma = \frac{\Delta P}{vL} \tag{9}$$

where ΔP is the air pressure difference across the test specimen subjected to an airflow of velocity v and thickness L. The standard requires test specimens of at least 90 mm in diameter and a velocity of 0.5 mm/s. In this work, since acoustic impedance tube measurements are performed on specimens of 44.44 mm in diameter, the same specimens were used for the airflow resistivity test at 0.5 mm/s.

To control the thickness and the diameter of the compacted fiber blend, the specimen holder shown in Figure 4 is used. A given mass M is carefully compacted in the inner volume of the specimen as homogeneously as possible. This fixes the bulk density of the fiber blend. For this density, the static airflow resistivity is measured with Equation 9. The measurement procedure is repeated for different compactions in the range ρ_B = [40, 180] kg/m^3;. The measured results are presented in Figure 5. As one can note, the relation between $\sigma(\rho_B)$ follows a power law growth. Since at $\sigma(0) = 0$ (i.e., air with $\phi = 1$) and $\sigma(\rho_f) = \infty$ (i.e., solid block with $\phi = 0$), the following relation is proposed

$$\sigma(\rho_B) = K_1 \left(\frac{\rho_B}{\rho_f - \rho_B} \right)^{K_2}. \tag{10}$$

with K_1 = 924 580 Nsm^{-4} and K^2 = 2.005 obtained from a simplex search method (function *fminsearch* in Matlab R2012b) with a coefficient of determination 0.9961. Using Equation 7, the previous relation can be rewritten as $\sigma(\rho_B) = K_1 (\phi\rho_f)^{-K_2} \rho_B^{K_2}$

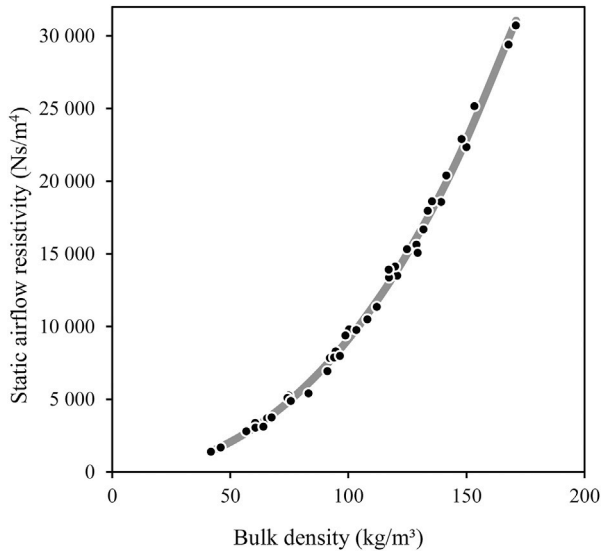

FIGURE 5
Static airflow resistivity versus the bulk density of the fiber blend. The dots are the measured data and the line is the power law regression with a coefficient of regression of 0.9961.

which is of a similar form to the one proposed by Bies and Hansen (Bies and Hansen, 1980) for fiberglass materials (i.e., $\sigma = 3.18 \times 10^{-9} d^{-2} \rho_B^{1.53}$, where d is the fiber diameter). This growth for fiberglass is smaller than the one of the RNF blend. This makes sense if one considers that recycled carpet fibers have a more sinuous shape than glass fibers. For the studied RNF blend, Equation 10 is preferred to a power law relationship including fiber diameter, because it has exact limits at low and high bulk densities.

3.6 Viscous (Λ) and thermal (Λ') characteristic lengths

The viscous and thermal characteristic lengths are two parameters used to accurately model the high-frequency viscous and thermal dissipations of sound waves in open-cell porous materials. The preferred measuring methods for these two parameters are based on ultrasound measurements (Leclaire et al., 1996). In this work, an inverse method using software Foam-X was chosen instead (Atalla and Panneton, 2005; ESI Group, 2024). This is due to the difficulty of having nicely shaped specimens for ultrasound measurements. The inverse method is based on impedance tube measurements. Typically, constrained by the physics of the sound propagation in porous media, the method iteratively searches the unknown parameters of a precursor acoustic model. The precursor model is the JCA model discussed in the Theory section. For a given 50-mm thick compacted RNF blend of bulk density ρ_B, the inversion solver is fed with the measured absorption coefficient, and the measured open porosity and resistivity. Consequently, the inversion solver searches the remaining macroscopic parameters of the blend, namely, the viscous and thermal characteristic lengths, and the tortuosity (discussed below).

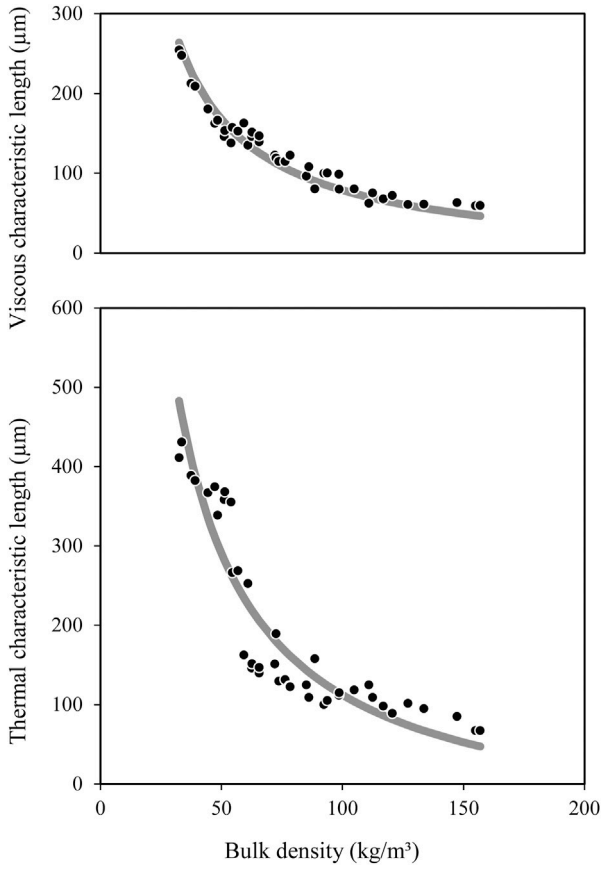

FIGURE 6
Viscous characteristic length (top) and thermal characteristic length (bottom) versus the bulk density of the fiber blend. The dots are the measured data and the lines are the curve fit models with coefficients of regression of 0.9158 and 0.8117, respectively.

Based on this procedure, several blends of different bulk densities were tested and their characteristic lengths were identified. The results are presented in Figure 6. Compared to static airflow resistivity measurements, the correlation between bulk density and characteristic lengths is lower. This shows the sensitivity of the inverse method to measurement errors of all input parameters (bulk density, open porosity, resistivity, absorption coefficient, thickness, precursor model). However, the correlation is clearly sufficient to propose an empirical model to relate the characteristic lengths to bulk density. Based on the work by Allard and Champoux (1992), when the interaction between fibers can be neglected (i.e., diluted fiber media where the distance between fibers is large compared to the fiber diameters), the following relationships hold for a diluted fiber perpendicular to the flow:

$$\Lambda = \frac{1}{\pi d l} \tag{11}$$

$$\Lambda' = 2\Lambda \tag{12}$$

where l is the length of fiber per unit volume of the fibrous aggregate. One recognizes that $\pi d^2 l/4$ is the solid phase volume (V_s) to total volume (V) ratio of the fibrous aggregate. This ratio is linked to the open porosity by $\phi = 1 - V_s/V$. Consequently, following this

observation, and making use of Equation 7, the viscous length in Equation 11 can be rewritten as:

$$\Lambda = \frac{d\rho_f}{4\rho_B}. \tag{13}$$

This indicates that the characteristic lengths are inversely proportional to the bulk density. Obviously, at high compaction levels, the diluted medium assumption may not hold anymore for the studied RNF blend, and one can assume that the condition on the characteristic lengths would be $\Lambda \leq \Lambda' \leq 2\Lambda$ (note that $\Lambda \leq \Lambda'$ is imposed by theory).

Following Equation 13 and the previous discussion, inverse relationships between the characteristic lengths and the bulk density can be found by a constrained minimization process with constraint $\Lambda \leq \Lambda' \leq 2\Lambda$. Applying such a minimization (function *fmincon* in Matlab R2012b) on the data presented in Figure 6 yields the following relationships

$$\Lambda(\rho_B) = \left(8.1718\frac{\rho_f}{\rho_B} - 10.8878\right) \times 10^{-6} \tag{14}$$

$$\Lambda'(\rho_B) = \left(16.3436\frac{\rho_f}{\rho_B} - 66.8678\right) \times 10^{-6} \tag{15}$$

with coefficients of regression of 0.9158 and 0.8117, respectively. At high values of the density ratio ρ_f/ρ_B (i.e., diluted fibers, $\phi \to 1$, see Equation 7), the first terms of Equations 14, 15 dominate and the diluted condition $\Lambda' = 2\Lambda$ of Equation 12 is found. One has to note that the previous relationships obtained from the constrained minimization process are valid for the studied range of bulk densities, and extrapolation to external values should be considered with care.

3.7 Tortuosity (α_∞)

Tortuosity is a parameter that indicates how the path of a sound wave in the porous medium deviates from a straight path. If the path is straight, $\alpha_\infty = 1$, else $\alpha_\infty > 1$. For diluted fibers, Allard and Champoux (1992) showed that $\alpha_\infty = 1$. This is the case for most fiberglass products. However, for dense fibrous materials (such as felts), the tortuosity may be larger.

The preferred method for measuring tortuosity is based on ultrasound techniques (Allard et al., 1994).[24] However, as discussed for the characteristic lengths, the inverse method was used to identify the tortuosity of the RNF blend at different compaction levels. The results are shown in Figure 7. One can note two different behaviors in function of the bulk density. Up to a value of 88 kg/m^3; corresponding approximately to a porosity of 0.92, the RNF blend can be considered as diluted in terms of tortuosity since $\alpha_\infty = 1$. However, for larger bulk densities, the tortuosity increases linearly with bulk density. This is logical because, as the fibers are closer, the path of the sound wave is increasingly perturbed. Consequently, the following empirical relationship between tortuosity and bulk density is proposed:

$$\alpha_\infty(\rho_B) = \begin{cases} 1 & \rho_B \leq 88 \text{ kg/m}^3 \\ 0.004\rho_B + 0.647 & \rho_B > 88 \text{ kg/m}^3 \end{cases}. \tag{16}$$

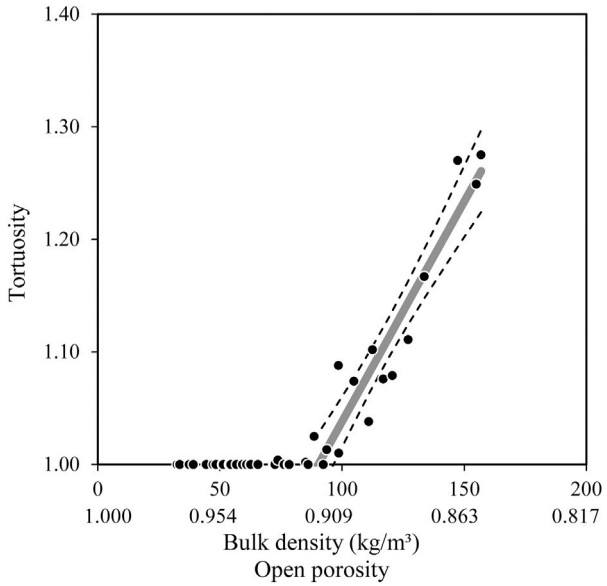

FIGURE 7
Tortuosity versus the bulk density (and corresponding open porosity) of the fiber blend. The dots are the measured data and the line is the curve fit model with coefficient of regression of 0.8952.

4 Semi-empirical model

The empirical relationships between the macroscopic parameters of the RNF blend and its bulk density developed in the previous section are valid for the studied range of RNF fiber blends. These empirical relationships (Equations 8, 10, 14–16) can be substituted into the JCA equivalent fluid model (Equations 2–4) to form a semi-empirical model. Doing so, the sound absorption coefficient, Equation 5, now depends on the frequency, the thickness, and bulk density of the NCF blend only: $\alpha(\rho_B, L, f)$.

To validate this semi-empirical model, three RNF blends of 30, 120 and 180 kg/m^3; are assembled and tested in the acoustical impedance tube described above. Validations are made for 50-mm thick samples. Note that densities 30 and 180 kg/m^3; are at the bounds of the range on which the empirical relationships were built. This will test the robustness of the model at its low and high limits. The sound absorption measurements are compared to the predictions obtained with the developed semi-empirical model in Figure 8. Three measurements are done for each density. Good correlations are obtained between the measurements and the predictions of the developed semi-empirical model.

5 Optimization procedure

From a noise control point of view, it is always desirable to have a simple solution that is tailored to a given problem. A design engineer would like to know the thickness to use for a given material to reach maximum sound absorption at a given frequency when it is backed by a hard wall. Alternatively, he could want to know the material to use for a fixed thickness to reach maximum absorption at a given frequency. To answer these questions, the engineer needs to test (or simulate when

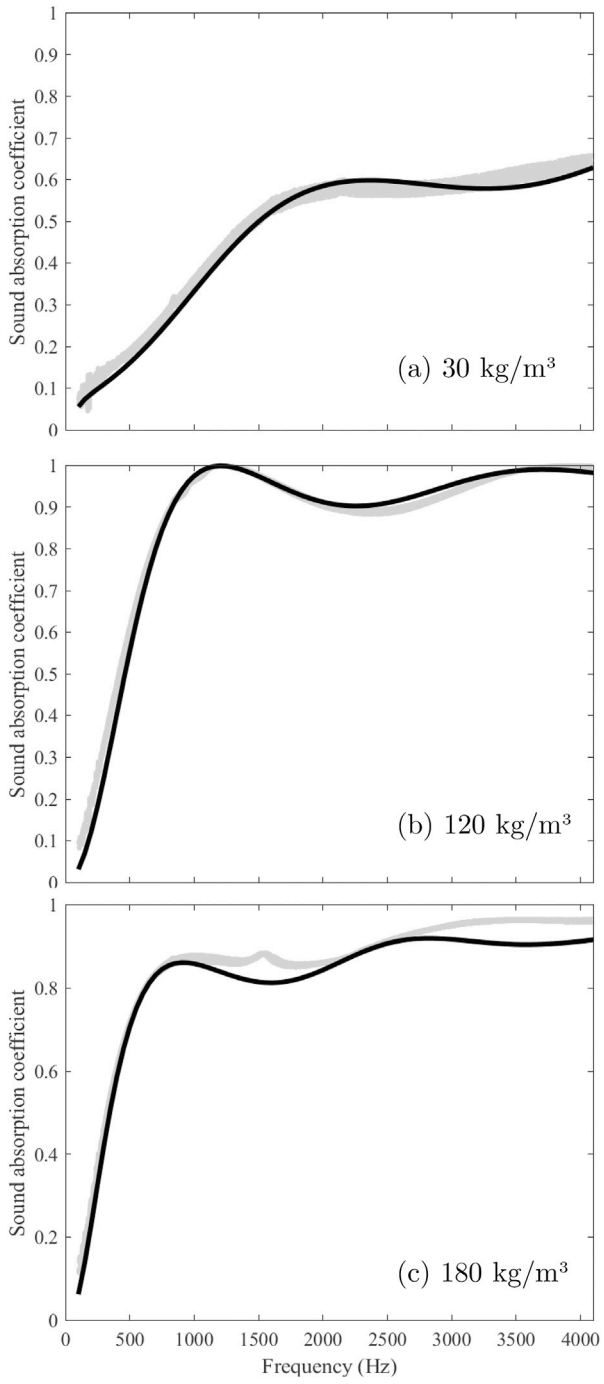

FIGURE 8
Sound absorption coefficient of three 50-mm thick RNF blend compactions: **(A)** 30 kg/m^3, **(B)** 120 kg/m^3, and **(C)** 180 kg/m^3. The black lines are the model predictions, and the gray areas show the dispersion of the measurements on three different specimens of the same compaction.

possible) different thicknesses, hoping to find the desired optimal solution. This process is lengthy and may yield no optimal results.

Another optimization process would be to adjust the 5 material parameters to reach a given objective. Such an approach is not realistic because the solution found could not make sense physically. In fact, all the parameters of the material are related to its microstructure. Apart from using a microstructural model and sophisticated simulation tools (Perrot et al., 2008; Tran et al., 2024b), one needs to perform a systematic study on the relationship between sound absorption and the material properties. In the past, some optimization studies on fibrous absorbers have been done. Shoshani and Yakubov (2000) made a numerical investigation to obtain optimal parameters for a sound-absorbing fiber web in terms of thickness, porosity, density and coupling parameter (function of resistivity). Their analysis did not take into account for the fact that the material parameters are linked together in a blend (e.g.,: porosity does not vary independently from resistivity, nor density). While their study gives interesting insights, it cannot be systematically applied in a real situation. More recently, Yang et al. (2011) investigated experimentally the effects of the bulk density on the sound-absorbing behavior of a fiber assembly at different compaction levels using a similar setup as the one used in Figure 3. They noticed that there exists an optimum density at which the sound absorption passes through a maximum at a so-called critical frequency. Nevertheless, they did not make a systematic optimization study to link the critical frequency and optimum density to the material properties and thickness. However, such a systematic study had already been made by Mechel (1988) to obtain design charts for fibrous sound absorbers. Based on a one-parameter equivalent fluid empirical model (here the parameter was resistivity), he observed that the sound absorption coefficient is governed by two non-dimensional parameters: $k_0 L$ and $\sigma L/Z_0$, where $k_0 = 2\pi f/c_0$ is the free field wavenumber in air. From this observation, he built design charts at different angles of incidence of the acoustic wave. The design charts can be used to find optimal values of thickness and resistivity to reach a maximum absorption at a given frequency. While his charts are of practical interest, they were built from a one-parameter empirical model valid for a given set of fibrous materials.

For the RNF blend under study, the developed semi-empirical model may be used to find the optimal parameters that will maximize the sound absorption of the blend when backed by a hard wall. This is possible since the only material parameter of the model is the bulk density. Once the optimal bulk density is found, the fiber blend is fully determined; there is no need to directly know what the 5 macroscopic parameters are. Consequently, the optimization process could be posed by one of the following expressions:

$$\begin{aligned} &\max_{\rho_B \in [30,180]} && \alpha(\rho_B, f_0, L) \\ &\max_{L \in [0,\infty]} && \alpha(\rho_B, f_0, L) \\ &\max_{\rho_B \in [30,180], L \in [0,\infty]} && \alpha(\rho_B, f_0, L) \end{aligned} \tag{17}$$

where f_0 is the frequency at which the absorption must reach a maximum. The difficulty in using directly Equation 17 lies in the frequency behavior of the absorption that can show several maxima. Another approach is inspired by the work of Mechel (1988) It consists of computing the normal incidence sound absorption coefficient $\alpha(\rho_B, L, f)$ from the developed semi-empirical model, and plotting absorption charts in function of the non-dimensional parameters $F = k_0 L$ and $R = \sigma L/Z_0$. Here, since the relationship is known between resistivity and bulk density, the second parameter is replaced by $\sigma(\rho_B)L/Z_0$, where $\sigma(\rho_B)$ is given by Equation 10. Such charts are given in Figure 9 for three different thicknesses: 25, 50, and 100 mm. The charts are similar to the normal incidence absorption chart obtained by Mechel. However, contrary to Mechel, a single chart is not sufficient to represent the studied materials. In fact, the absorption chart also depends on the

10.3389/facou.2024.1478414

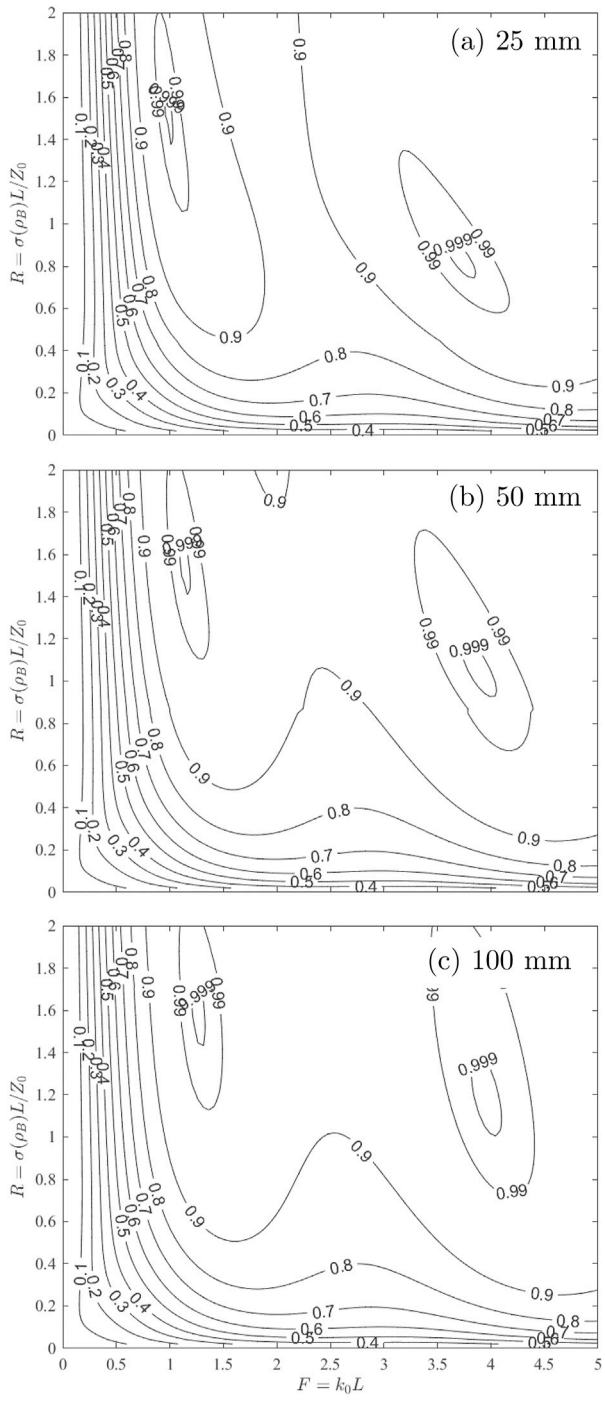

FIGURE 9
Sound absorption charts as a function of the two non-dimensional parameters *R* and *F* for different thicknesses of the RNF blend: **(A)** 25, **(B)** 50, and **(C)** 100 mm.

thickness, and not only on *R* and *F*. This is explained by the fact the studied material cannot be described by the resistivity only, as in the empirical model by Mechel. This supports the choice of using the more complex and general five-parameter JCA model to build our semi-empirical model.

For each chart in Figure 9, one notes that more than one maximum exists. The first maximum occurs at the so-called critical frequency f_1 For this frequency, one can clearly determine the optimal non-dimensional parameters *R* and *F*. One can note that the optimal value for *R* is slightly influenced by the thickness. For the three thicknesses, its optimal values are 1.47, 1.57 and 1.57, respectively. For a thickness of 50 mm and Z_0 = 414 Nsm^{-3}, this yields an optimal resistivity of 12 986 Nsm^{-4} or, using Equation 10, an optimal bulk density of 116 kg/m^3;. As for the non-dimensional parameter *F*, one can note that its optimal value increases with the thickness. For 25, 50, and 100 mm, the optimal values of *F* are 1.00, 1.12 and 1.27, respectively. For a thickness of 50 mm and c_0 = 343 m/s, this yields an optimal frequency of 1,224 Hz. As demonstrated, the charts in Figure 9 can be used to quickly identify a configuration yielding maximum absorption. However, if the thickness has to be fixed to a value not given in Figure 9, one needs to interpolate.

Another, more straightforward, approach is to identify relationships between the bulk density, the thickness and the critical frequency at which the first maximum of sound absorption occurs. To proceed this way, one can obtain the sound absorption coefficient for a range of admissible bulk densities and thicknesses on which the empirical relations were built in the previous section. Here, the sound absorption coefficient $\alpha(\rho_B, L, f)$ is computed for the following admissible combinations: ρ_B = 30: 2: 180 kg/m^3;, L = 10: 10: 250 mm, and $k_0 L$ = 0: 0.01: 2.5. For each thickness, the optimal bulk density ρ_B^{opt} is identified together with the optimal non-dimensional parameter $|k_e L|_{opt}$ at which the first maximum of sound absorption occurs. Here, k_e is the complex wave number in the material. These optimal absorption behaviors are plotted in Figure 10 in function of $k_0 L$ and $|k_e L|$. One notes that for all thicknesses, the maximum absorption occurs around the non-dimensional parameter $(k_0 L)_{opt} \approx 1.30$ or $|k_e L|_{opt} \approx 2.04$. The ratio between these two optimal parameters, $r_{p\to a} = (k_0 L)_{opt}/|k_e L|_{opt} \approx 0.62$, can be viewed as a projection factor from the porous material wavenumber domain to the air wavenumber domain.

The identified optimal value $|k_e L|_{opt} \approx 2.04$ may also be found theoretically. In fact, for a sound absorbing material of thickness *L* backed by a hard wall, the maximum absorption is mainly reached when the maximum viscous dissipation is reached. This maximum dissipation occurs approximately when the squared RMS acoustic velocity in the material is maximum. Under a normal incidence plane wave, if the origin of the *x*-axis is at the hard wall, the squared RMS acoustic velocity in the material is given by

$$v_{RMS}^2 = \left| \frac{4A^2}{Z_e^2 L} \int_0^L \sin(k_e x)^2 dx \right| \tag{18}$$

where *A* is the amplitude of the pressure wave in the material, $Z_e = \sqrt{\rho_e K_e}$ and $k_e = 2\pi f \sqrt{\rho_e / K_e}$ are the characteristic impedance and wave number in the material. The maximum of Equation 18 occurs at optimal non-dimensional parameter $k_e L = |k_e L|_{opt} \approx 2.2$, which is about the one found from the simulations. This value is an approximation and depends also on the thermal losses and material properties.

From the previous simulations and discussions, it is clear that a relationship exists between ρ_B^{opt} and $|k_e L|_{opt}$. Moreover, for a given thickness, $|k_e L|_{opt}$ yields the critical frequency at which the first maximum peak occurs:

$$f_1^p = \frac{c_0}{2\pi} \frac{|k_e L|_{opt}}{L} \approx \frac{112}{L} \tag{19}$$

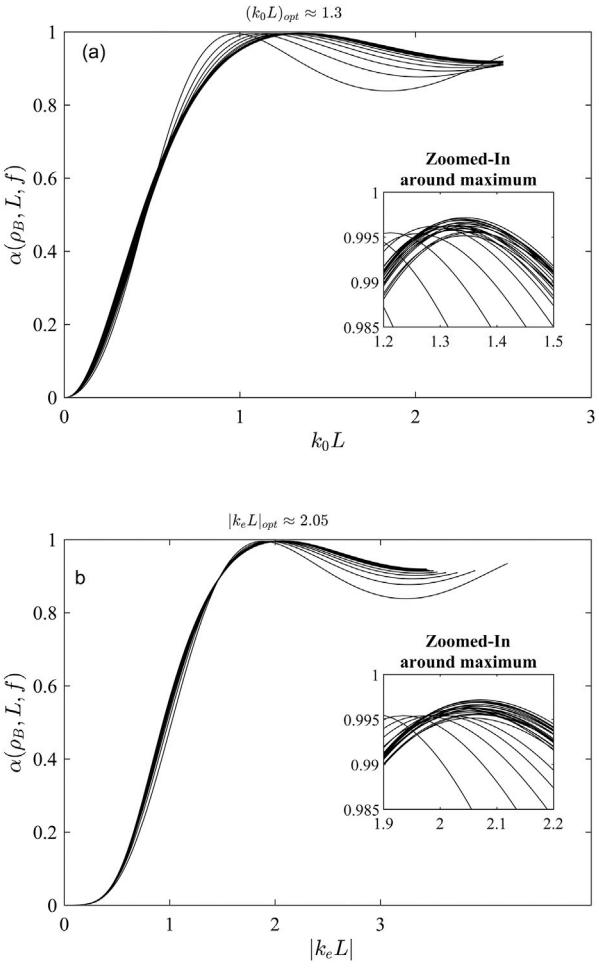

FIGURE 10
Normal incidence hard backed sound absorption coefficient of the RNF blend in function of non-dimensional parameter **(A)** k_0L (top) and **(B)** $|k_eL|$ (bottom) at the optimal bulk density $\rho_B^{opt}(L)$ for each thickness L ranging from 10 to 250 mm.

with c_0 = 343 m/s at standard atmospheric conditions. The previous frequency is in the porous material wavenumber domain. To obtain its value in the air wavenumber domain, the following conversion is needed:

$$f_1^a = r_{p\to a} f_1^p \tag{20}$$

with $r_{p\to a} \approx 0.62$. From the simulation results, the relationships between these parameters are plotted in Figure 11 for the calculated thicknesses. Also the following power law is obtained for the optimal bulk density:

$$\rho_B^{opt} = \frac{27.958}{L^{0.437}} \tag{21}$$

6 Application of the optimization procedure

In the following, Equations 19–21 will be used to find the optimal RNF blend for different sound absorber design objectives.

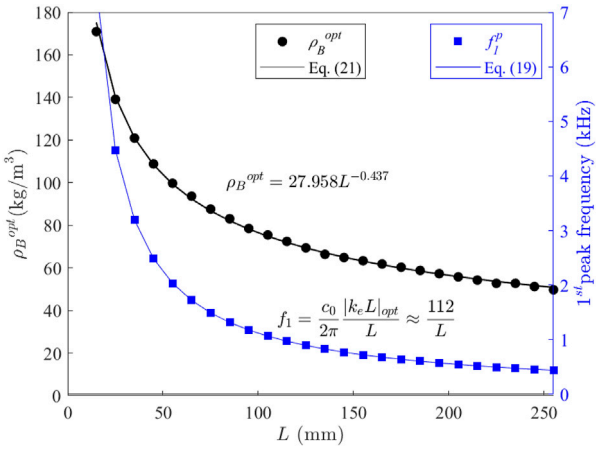

FIGURE 11
Optimal bulk density $\rho_B^{opt}(L)$ and first absorption peak frequency f_1 in function of the thickness. These curves are valid for normal incidence hard backed sound absorption coefficient.

6.1 Find optimal configuration for maximum absorption at 500 Hz

To find this optimal configuration for f_1^a = 500 Hz, Equation 20 is first used to convert the frequency in the porous material wavenumber domain; this yields f_1^p = 806 Hz. Then, Equation 19 is used to find the corresponding thickness; this yields L = 139 mm. From this thickness, one find the optimal bulk density from Equation 21, which yields ρ_B^{opt} = 66 kg/m^3;. Figure 12A compares the measured sound absorption coefficient for this configuration with the model prediction. One can observe the optimization proceeds correctly.

6.2 Find optimal bulk density for a thickness of 50 mm

To find this configuration, Equation 21 is first used to find the optimal bulk density; this yields ρ_B^{opt} = 104 kg/m^3;. Equations 19, 20 are used to obtain the frequency of the first peak in the air domain; this yields f_1^a = 1389 Hz. Figure 12B compares the measured sound absorption coefficient for this configuration with the model prediction. One can observe the optimization perfectly fits with the objective.

6.3 Find optimal thickness for an optimal density of 140 kg/m^3

To find this configuration, Equation 21 is first used to find the thickness; this yields L = 25 mm. Then, Equations 19, 20 are used to obtain the frequency of the first peak in the air domain; this yields f_1^a = 2778 Hz. Figure 12C compares the measured sound absorption coefficient for this configuration with the model prediction. Again, the optimization worked fine.

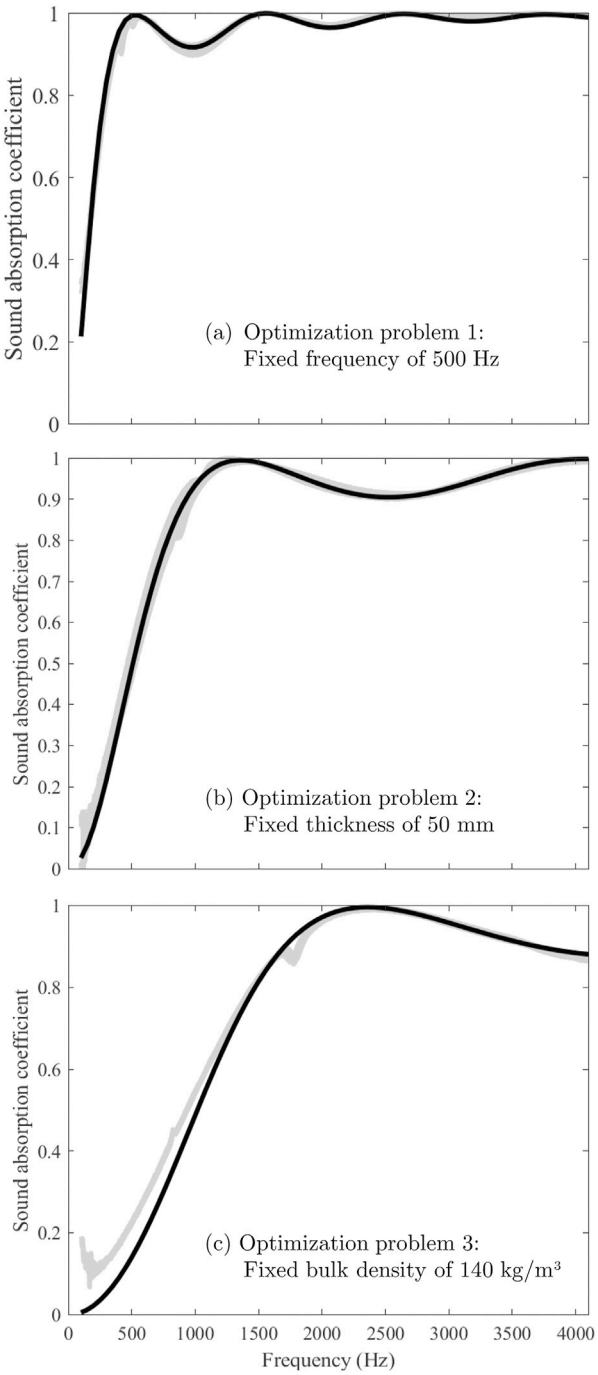

FIGURE 12
Normal incidence hard backed sound absorption coefficient. **(A)** Optimization problem 1 with fixed frequency of 500 Hz; **(B)** Optimization problem 2, with fixed thickness of 50 mm; **(C)** Optimization problem 3, with fixed bulk density of 140 kg/m^3. The black lines are the model predictions, and the gray areas show the dispersion of the measurements on three different specimens of the same compaction.

7 Conclusion

In this paper, a semi-empirical model was derived to predict the normal incidence sound absorption coefficient of a Recycled Nylon Fiber (RNF) blend. The semi-empirical model is based on the general five-parameter Johnson-Champoux-Allard (JCA) for porous materials in which the five parameters (i.e., open porosity, airflow resistivity, tortuosity, viscous and thermal characteristic lengths) are replaced by characterized empirical relationships expressed in terms of the bulk density of the blend only. From this semi-empirical model, sound absorption charts were built to help design optimized RNF absorbers. A more systematic design procedure based on equations was also worked out. The procedure allows for a quick determination of the optimal parameters of a mixture to achieve maximum absorption. Three design problems were addressed and validated by experiments 1) to determine the optimal thickness and bulk density to reach maximum absorption at a given frequency, 2) to find the optimal density for a given thickness, and 3) to find the optimal thickness for a given bulk density. While the optimization procedure was developed for RNF absorbers, a similar procedure could be developed for any other fibrous-like sound absorbers. More specifically, the proposed method could be applied to cotton felts which have smaller fiber diameters and are often used in the automotive industry. This could be a simpler way to optimize these felts for sound absorption compared to a complex multi-scale analysis as done elsewhere (Tran et al., 2024b).

Data availability statement

The raw data supporting the conclusions of this article will be made available by the authors, without undue reservation.

Author contributions

JB: Conceptualization, Data curation, Formal Analysis, Investigation, Methodology, Validation, Visualization, Writing–original draft, Writing–review and editing. SE: Conceptualization, Formal Analysis, Methodology, Resources, Supervision, Writing–original draft. RP: Conceptualization, Formal Analysis, Funding acquisition, Methodology, Project administration, Resources, Software, Supervision, Visualization, Writing–original draft, Writing–review and editing.

Funding

The author(s) declare that financial support was received for the research, authorship, and/or publication of this article. The authors acknowledge the financial support of Natural Sciences and Engineering Research Council (NSERC) [funding reference numbers: RGPIN-2018–06113 and RGPIN-2019–06573]. We also extend our gratitude to RECYC-QUÉBEC for awarding a scholarship to Julien Biboud for his master's research.

Acknowledgments

The authors thank Leigh Textile and Jasztex for providing materials.

Conflict of interest

Author JB was employed by Mecanum Inc.

The remaining authors declare that the research was conducted in the absence of any commercial or financial relationships that could be construed as a potential conflict of interest.

Publisher's note

References

Allard, J., and Atalla, N. (2009). *Propagation of sound in porous media: modelling sound absorbing materials*. John Wiley & Sons.

Allard, J. F., Castagnede, B., Henry, M., and Lauriks, W. (1994). Evaluation of tortuosity in acoustic porous materials saturated by air. *Rev. Sci. Instrum.* 65, 754–755. doi:10.1063/1.1145097

Allard, J.-F., and Champoux, Y. (1992). New empirical equations for sound propagation in rigid frame fibrous materials. *J. Acoust. Soc. Am.* 91, 3346–3353. doi:10.1121/1.402824

Asdrubali, F. (2006). Survey on the acoustical properties of new sustainable materials for noise control. *Proc. Euronoise Eur. Acoust. Assoc. Tampere* 30, 1–10.

Atalla, Y., and Panneton, R. (2005). Inverse acoustical characterization of open cell porous media using impedance tube measurements. *Can. Acoust.* 33, 11–24.

Bies, D., and Hansen, C. H. (1980). Flow resistance information for acoustical design. *Appl. Acoust.* 13, 357–391. doi:10.1016/0003-682x(80)90002-x

D'Alessandro, F., and Pispola, G. (2005). Sound absorption properties of sustainable fibrous materials in an enhanced reverberation room. *INTER-NOISE NOISE-CON Congr. Conf. Proc. Inst. Noise Control Eng.* 2005, 2209–2218.

Delany, M. E., and Bazley, E. (1970). Acoustical properties of fibrous absorbent materials. *Appl. Acoust.* 3, 105–116. doi:10.1016/0003-682x(70)90031-9

Del Rey, R., Alba, J., Ramis, J., and Sanchís, V. (2011). Nuevos materiales absorbentes acústicos obtenidos a partir de restos de botellas de plástico. *Mater. construcción* 61, 547–558. doi:10.3989/mc.2011.59610

Desarnaulds, V., Costanzo, E., Carvalho, A., and Arlaud, B. (2005). "Sustainability of acoustic materials and acoustic characterization of sustainable materials," in *Proceedings of the 12th international congress on sound and vibration*.

ESI Group (2024). FOAM-X software. Standalone utility for characterizing the Biot properties of open-cell porous materials based on impedance tube measurements. *Software*.

ISO 10534-2:2023 (2023). *Acoustics — determination of acoustic properties in impedance tubes—Part 2: two-microphone technique for normal sound absorption coefficient and normal surface impedance*. Standard: International Organization for Standardization.

ISO 9053-2:2020 (2020). *Acoustics — determination of airflow resistance—Part 2: alternating airflow method*. Standard: International Organization for Standardization.

Kosuge, K., Takayasu, A., and Hori, T. (2005). Recyclable flame retardant nonwoven for sound absorption; RUBA®. *J. Mater. Sci.* 40, 5399–5405. doi:10.1007/s10853-005-4338-9

Langley, K. D., Kim, Y. K., and Lewis, A. F. (2000). *Recycl. reuse mixed-fiber Fabr. remnants:spandex, cotton & Polyest. UMass Lowell, Chelsea Cent. Recycl. Econ. Dev.*

Leclaire, P., Kelders, L., Lauriks, W., Melon, M., Brown, N., and Castagnede, B. (1996). Determination of the viscous and thermal characteristic lengths of plastic foams by ultrasonic measurements in helium and air. *J. Appl. Phys.* 80, 2009–2012. doi:10.1063/1.363817

Lee, Y., and Joo, C. (2003). Sound absorption properties of recycled polyester fibrous assembly absorbers. *AUTEX Res. J.* 3, 78–84. doi:10.1515/aut-2003-030205

Lei, L., Dauchez, N., and Chazot, J. (2018). Prediction of the six parameters of an equivalent fluid model for thermocompressed glass wools and melamine foam. *Appl. Acoust.* 139, 44–56. doi:10.1016/j.apacoust.2018.04.010

Lorenzana, M. T., Dafonte, P., Rilo, E., Cabeza, O., and González, J. (2002). "Absorbent characteristics of materials obtained from industrial wastes," in *Proc. Of forum acusticum, seville, Spain*.

Luu, H. T., Perrot, C., and Panneton, R. (2017). Influence of porosity, fiber radius and fiber orientation on the transport and acoustic properties of random fiber structures. *ACTA Acustica united Acustica* 103, 1050–1063. doi:10.3813/aaa.919134

Maderuelo-Sanz, R., Nadal-Gisbert, A. V., Crespo-Amorós, J. E., and Parres-García, F. (2012). A novel sound absorber with recycled fibers coming from end of life tires (elts). *Appl. Acoust.* 73, 402–408. doi:10.1016/j.apacoust.2011.12.001

Manning, J., and Panneton, R. (2013). Acoustical model for shoddy-based fiber sound absorbers. *Text. Res. J.* 83, 1356–1370. doi:10.1177/0040517512470196

Mechel, F. (1988). Design charts for sound absorber layers. *J. Acoust. Soc. Am.* 83, 1002–1013. doi:10.1121/1.396045

Panneton, R. (2007). Comments on the limp frame equivalent fluid model for porous media. *J. Acoust. Soc. Am.* 122, EL217–EL222. doi:10.1121/1.2800895

Perrot, C., Chevillotte, F., and Panneton, R. (2008). Bottom-up approach for microstructure optimization of sound absorbing materials. *J. Acoust. Soc. Am.* 124, 940–948. doi:10.1121/1.2945115

Piégay, C., Glé, P., Gourlay, E., Gourdon, E., and Marceau, S. (2021). A self-consistent approach for the acoustical modeling of vegetal wools. *J. Sound Vib.* 495, 115911. doi:10.1016/j.jsv.2020.115911

Pompoli, F., and Bonfiglio, P. (2020). Definition of analytical models of non-acoustical parameters for randomly-assembled symmetric and asymmetric radii distribution in parallel fiber structures. *Appl. Acoust.* 159, 107091. doi:10.1016/j.apacoust.2019.107091

Salissou, Y., and Panneton, R. (2007). Pressure/mass method to measure open porosity of porous solids. *J. Appl. Phys.* 101. doi:10.1063/1.2749486

Santoni, A., Bonfiglio, P., Fausti, P., Marescotti, C., Mazzanti, V., Mollica, F., et al. (2019). Improving the sound absorption performance of sustainable thermal insulation materials: natural hemp fibres. *Appl. Acoust.* 150, 279–289. doi:10.1016/j.apacoust.2019.02.022

Shoshani, Y., and Yakubov, Y. (2000). Numerical assessment of maximal absorption coefficients for nonwoven fiberwebs. *Appl. Acoust.* 59, 77–87. doi:10.1016/s0003-682x(99)00015-8

Tran, Q. V., Perrot, C., Panneton, R., Hoang, M. T., Dejaeger, L., Marcel, V., et al. (2024a). Effect of polydispersity on the transport and sound absorbing properties of three-dimensional random fibrous structures. *Int. J. Solids Struct.* 296, 112840. doi:10.1016/j.ijsolstr.2024.112840

Tran, Q. V., Perrot, C., Panneton, R., Hoang, M. T., Dejaeger, L., Marcel, V., et al. (2024b). Utilizing polydispersity in three-dimensional random fibrous based sound absorbing materials. *Mater. Des.* 247, 113375. doi:10.1016/j.matdes.2024.113375

Yang, S., Yu, W., and Pan, N. (2011). Investigation of the sound-absorbing behavior of fiber assemblies. *Text. Res. J.* 81, 673–682. doi:10.1177/0040517510385177